NOVEMBER 1974 MATT-1084

ENERGY TRANSPORT ACROSS A MAGNETIC FIELD BY PLASMA WAVES

BY

JOSÉ CANOSA AND HIDEO OKUDA

PLASMA PHYSICS LABORATORY

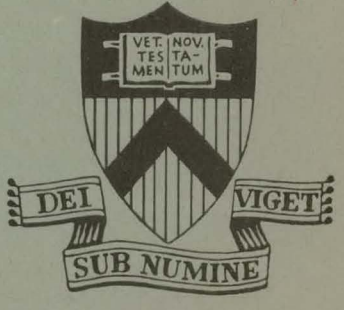

PRINCETON UNIVERSITY
PRINCETON, NEW JERSEY

This work was supported by U. S. Atomic Energy Commission Contract AT(11-1)-3073. Reproduction, translation, publication, use, and disposal, in whole or in part, by or for the United States Government is permitted.

DISCLAIMER

Energy Transport Across a Magnetic Field by Plasma Waves

José Canosa* and Hideo Okuda

Plasma Physics Laboratory, Princeton University

Princeton, New Jersey 08540

ABSTRACT

Cross-field energy transport by electrostatic plasma waves has been studied theoretically and numerically for a plasma near thermal equilibrium. Energy transfer by plasma waves is significant in a high temperature plasma where collisional transport is quite small. For strong magnetic fields ($\omega_c \gtrsim \omega_p$), the simulations verify the theoretical prediction that energy transport by plasma waves increases slowly with the magnetic field, and that in the limit of large field magnitudes wave transport dominates classical collisional transport. Furthermore, in a strong magnetic field the relaxation of the temperature by wave transport may result in an anisotropic velocity distribution. For weak fields ($\omega_p > \omega_c$), the simulation shows that collisional transport is more important than wave transport, also in agreement with the theory.

I. INTRODUCTION

The study of plasma confinement in a strong magnetic field has been one of the main goals of the controlled thermonuclear research program. As is well known, the classical theory of plasma transport almost always fails to explain the experimentally observed rapid loss of particles and heat in many of the confining devices. The rapid losses are assumed implicitly to be due to some kind of plasma instability which causes turbulent transfer.

Recently, it has been pointed out[1,2] that in addition to classical processes, there is a large transport of particles and heat due to low-frequency electrostatic fluctuations, even in thermal equilibrium. These thermal convective cells are created by low-frequency fluctuations across the magnetic field which transport particles very easily by the c $\underline{E}$ x $\underline{B}/B^2$ drift. Furthermore, it has also been found[2] that low frequency ion fluctuations near the lower hybrid frequency can cause large electron transport across the magnetic field. In addition to these energy transport mechanisms, Rosenbluth and Liu[3] have shown recently that electrostatic waves can carry an appreciable amount of energy across a strong magnetic field in a high temperature collisionless plasma. While the particles are not able to move easily across strong magnetic fields, there is a net flux of energy from the plasma center toward the boundaries associated with the spontaneous emission and absorption of electrostatic waves which propagate at arbitrary angles with respect to the magnetic field; this is because the amplitude of the thermal fluctuations is determined by the local temperature.

In this paper, we report on a theoretical and numerical study of energy transport across a magnetic field by electrostatic waves in a plasma near thermal equilibrium. In Section II, we obtain asymptotic forms of the dispersion relation for electrostatic waves both in the strong and weak magnetic field limits; these results are the foundation of the theory of wave energy transport. In Section III, we extend the work of Rosenbluth and Liu, and give a theory that describes explicitly and in some detail the influence of the magnetic field magnitude and of the plasma size on the energy transport. After a description of the numerical model used, in Section IV, we give the results of the numerical simulation of wave energy transport performed with a 2 1/2-dimensional particle code. The agreement between theory and simulation is quite satisfactory. We wish to emphasize that, although the present simulations are for a plasma near thermal equilibrium, it is straightforward to extend them to the more important case of a weakly turbulent plasma, such as those existing in present tokamak devices. Throughout the paper, it is assumed that the ions form an immobile uniform background.

II. DISPERSION RELATIONS FOR ELECTROSTATIC WAVES IN A MAGNETIC FIELD

The theory of plasma energy transport across a magnetic field by electrostatic plasma waves is based on a detailed knowledge of the dispersion properties of these waves. In this section, we obtain, therefore, asymptotic forms of the dispersion relation both in the strong and weak magnetic field limits.

For fixed ion background, no drift velocity, and an isotropic Maxwellian distribution, the dispersion equation for electrostatic waves in a magnetic field reduces to[4]

$$K^2 + 1 + i\pi^{1/2}\, zw(z) + \sum_{n=-\infty}^{\infty}{}' (1/|n|!)(\lambda/2)^{|n|}\left[1 + i\pi^{1/2}\, zw(z + nz_c)\right] = 0 , \quad (1)$$

where the prime means that the n = 0 term is not included in the sum, $K = k\lambda_D$ (k is the wavenumber and λ_D is the Debye length), w(z) is the function related to the complex error function and the plasma dispersion function,[5] z is the dimensionless complex frequency defined by

$$z \equiv \omega/2^{1/2}\, k_{\parallel} v_e , \quad (2)$$

and z_p and z_c are the dimensionless electron plasma and cyclotron frequencies. In the derivation of (1), we used the asymptotic approximations valid for small λ , $I_n(\lambda) \sim (1/n!)(\lambda/2)^n$, and $\exp(-\lambda) \sim 1$, where I_n are the Bessel functions, λ is the parameter for the finite gyroradius

$$\lambda \equiv k_{\perp}^2\, v_e^2/\omega_c^2 = k^2 \sin^2\theta\, v_e^2/\omega_c^2 , \quad (3)$$

and θ is the angle between the magnetic field and the wave vector. It should be noted that for parallel propagation, $k_{\parallel}$ in (2) becomes k , and $\lambda = 0$, so that Eq. (1)

becomes identical to Landau's dispersion equation,[6,7] as it should.

A. Strong Magnetic Field Limit

In this case, the main damping is due to the term with $w(z)$ in (1); therefore, we use the asymptotic expansion of $w(z \pm z_c)$ for large values of the argument and keep only the first term, i.e., $w(z \pm z_c) \sim (i/\pi^{1/2})(z \pm z_c)^{-1}$. In this way, (1) becomes

$$K^2 + 1 + i\pi^{1/2}\, zw(z) + K^2 \sin^2\theta\, z_p^2/(z_c^2 - z^2) \ . \qquad (4)$$

As $z_c^2 >> z^2$, Eq. (4) can be approximated by

$$K^2 + 1 + i\pi^{1/2}\, zw(z) + K^2 \sin^2\theta\, z_p^2/z_c^2 = 0 \ . \qquad (5)$$

Defining the parameter

$$K_m^2 \equiv K^2(1 + \sin^2\theta\, z_p^2/z_c^2) \equiv K^2 a \ , \qquad (6)$$

we can write (5) in exactly the same form as Landau's dispersion equation

$$K_m^2 + 1 + i\pi^{1/2}\, zw(z) = 0 \ , \qquad (7)$$

whose fifth-order solution in the long wavelength limit $K \to 0$ is of the same form as for the magnetic field free case,[8] once K is substituted by K_m . Transforming back to physical variables by using (2), the second-order solution of (7) is

$$\omega = \frac{\omega_p \cos\theta}{a^{1/2}}\left(1 + \frac{3}{2}K^2 a\right) - i\left(\frac{\pi}{8}\right)^{1/2}\frac{\omega_p \cos\theta}{a^{1/2}}\frac{1}{K^3 a^{3/2}}$$

$$\times \exp(-1/2a\ K^2)\cdot\exp(-3/2) \quad ,$$

$$a \equiv 1 + (\omega_p^2/\omega_c^2)\sin^2\theta \quad . \tag{8}$$

It should be noted that in the very strong magnetic field limit $\omega_c \to \infty$, $a \to 1$, and (8) adopts still a simpler form.

B. Weak Magnetic Field Limit

It is known that for weak magnetic fields, $z_c < z_p$, the Landau damping of electrostatic waves propagating in particular directions relative to the magnetic field can be orders of magnitude higher than the field-free Landau damping.[9] The dispersion equation (1) is solved as follows. To obtain the real part of the solution, we approximate (1) by keeping only the $n = \pm 1$ terms in the sum. In this way, we again obtain (4).

For weak magnetic fields, $z_c^2 << z^2$, and the fraction in the last term of (4) can be expanded as follows:

$$\frac{z_p^2}{z_c^2 - z^2} = - \frac{z_p^2}{z^2(1 - z_c^2/z^2)} \sim - \frac{z_p^2}{z^2}\left(1 + \frac{z_c^2}{z^2}\right) , \qquad (9)$$

so that (4) becomes

$$K^2 + 1 + i\,\pi^{1/2}\, z\, w(z) - K^2 \sin^2\theta\, \frac{z_p^2}{z^2}\left(1 + \frac{z_c^2}{z^2}\right) = 0 . \qquad (10)$$

In the long wavelength limit $K \to 0$, the well-known asymptotic expansion of $w(z)$ valid for large z gives[6,8]

$$K^2 - \frac{1}{2z^2} - \frac{3}{4z^4} \cdots - K^2 \sin^2\theta\, \frac{z_p^2}{z^2}\left(1 + \frac{z_c^2}{z^2}\right) = 0 , \qquad (11)$$

where the exponential term has been neglected as we are only solving for the real part. If the term $z_c^2/z^2 << 1$ inside the parentheses is dropped, we get a first-order approximation to the real part, $z^2 \sim z_p^2$. Letting $1 + z_c^2/z^2 \sim 1 + z_c^2/z_p^2$ in (11), we get after a little rearrangement

$$K^2 - \frac{b}{2z^2} - \frac{3}{4z^4} \cdots = 0 ,$$

$$b \equiv \frac{1}{\cos^2\theta}\left(1 + \frac{z_c^2}{z_p^2}\sin^2\theta\right) . \qquad (12)$$

Equation (12) is again in exactly the same form as the algebraic part of the field-free Landau's dispersion equation for long wavelengths, except that now there is the parameter b in the second term of (12) instead of 1 in Landau's equation.[8] The second-order solution for the real part is obtained as before,[8] and transforming back to physical variables with the use of (2), we get

$$\omega = \omega_p \left(1 + \frac{1}{2} \frac{\omega_c^2}{\omega_p^2} \sin^2 \theta + \frac{3}{2} K^2 \cos^4 \theta\right) . \tag{13}$$

Once the real part has been found, the imaginary part is obtained by substituting z by its real part in the exponential terms arising from the asymptotic expansions of the w functions in (1). After transforming back to physical variables by using (2), and further approximating $\omega \sim \omega_p$ in the imaginary part, we get[9]

$$\omega = \omega_p \left(1 + \frac{1}{2} \frac{\omega_c^2}{\omega_p^2} \sin^2 \theta + \frac{3}{2} K^2 \cos^4 \theta\right)$$

$$- i\left(\frac{\pi}{8}\right)^{1/2} \frac{\omega_p}{K^3 \cos \theta} \sum_{n=-\infty}^{\infty} \frac{(\lambda/2)^{|n|}}{|n|!} \exp\left[(-1/2K^2 \cos^2 \theta)\right.$$

$$\left. \times (\omega_p - n\omega_c)^2/\omega_p^2\right] . \tag{14}$$

For a given ω_p/ω_c, Ingvesson and Perkins[9] have shown that the most important term in the sum in (14) is that where n

is the smallest integer closest to ω_p/ω_c . This can be seen because the argument of the corresponding exponential is then the smallest. Therefore, we have finally

$$\omega \sim \omega_p\left(1+\frac{1}{2}\frac{\omega_c^2}{\omega_p^2}\sin^2\theta+\frac{3}{2}K^2\cos^4\theta\right)$$

$$- i(\pi/8)^{\frac{1}{2}} \frac{1}{n!}\frac{\omega_p}{K^3\cos\theta}(\lambda/2)^n ,$$

$$\lambda \equiv k_\perp^2 v_e^2/\omega_c^2 , \qquad (15)$$

where for simplicity we have assumed that the ratio ω_p/ω_c is sufficiently close to the integer n, so that the exponential term in (14) can be approximated by unity. As noted by Ingvesson and Perkins,[9] the Landau damping given by (15) might be orders of magnitude higher than the field-free Landau damping for intermediate values of the angle θ.[9]

III. THEORY OF ENERGY TRANSPORT BY PLASMA WAVES

Rosenbluth and Liu[3] have discussed recently the energy transport across a magnetic field by the spontaneous emission

and absorption by Landau damping of high frequency, long mean-free path plasma waves. They obtained asymptotic results valid in the limits $\omega_c >> \omega_p$ and $L >> \lambda_D$, where L is the half-width of the plasma slab. Their main conclusion is that this mechanism of energy transport is independent of the magnetic field magnitude and will dominate classical thermal diffusion in very large systems.

Our interest here is to develop a theory that can be subject to verification by computer simulation. This requires that we consider explicitly and in detail the influence of the magnetic field magnitude and of the plasma size on the energy transport. We have thus extended Rosenbluth and Liu's treatment and obtained more general results that approach asymptotically their results in the limits $\omega_c/\omega_p \to \infty$ and $L/\lambda_D \to \infty$. In the strong magnetic field case, $\omega_c > \omega_p$, our second-order calculation gives an energy loss which is significantly higher than that obtained by the first-order calculation,[3] even for large plasmas. We also find that the energy transport by plasma waves increases slowly with the magnetic field. In the weak magnetic field case, $\omega_c \leq \omega_p$, the energy loss by plasma waves is almost independent of its magnitude, and approaches the level due to wave absorption in the absence of magnetic field.

A. Strong Magnetic Field Limit

We first give the second-order calculation of the energy loss in the case $\omega_c/\omega_p > 1$. The treatment is based on that

given by Rosenbluth and Liu.[3] The transport equation for the electrostatic energy per mode in thermal equilibrium steady state is

$$\frac{dE}{dx} + \lambda(x)E = \lambda(x)T(x)$$

$$E(-L) = 0 \ . \tag{16}$$

The boundary condition in (16) is the reflective boundary condition for electrostatic waves, as these cannot escape the plasma. Here we consider a two-dimensional slab plasma in order to compare the theoretical results with those obtained from a 2 1/2-dimensional particle simulation. Thus, the magnetic field is $\underline{B} = B\hat{y}$, and the steady electron temperature is given by $T(x) = T_o(1 - x^2/L^2)$, where L is the plasma half-width. The absorption probability per unit length is given by $\lambda(x) = 2\gamma_L/v_x$, where γ_L is Landau's damping coefficient given by (8), and v_x is the group velocity

$$v_x = \frac{d(\mathrm{Re}\ \omega)}{dk_x} = \omega_p \frac{k_x k_y}{k^3 a^{1/2}} \left(1 - \varepsilon \cos^2\theta + \frac{9}{2} k^2 \lambda_D^2\right) ,$$

$$a \equiv 1 + \varepsilon \sin^2\theta \ , \quad \varepsilon \equiv \omega_p^2/\omega_c^2 \ , \tag{17}$$

obtained using the real part of the dispersion relation (8), and having approximated $a \approx 1$ inside the parentheses. Taking into account the temperature gradient in the strongly dominant exponential term of Landau's coefficient, we get explicitly for the absorption probability

$$\lambda(x) = \frac{2\gamma_L}{v_x} = \left(\frac{\pi}{2}\right)^{1/2} \frac{1}{4.5} \frac{1}{\lambda_D} \frac{1}{k_x k \lambda_D^2} \frac{1}{a^{3/2}} \left(1 + \varepsilon \cos^2\theta - \frac{9}{2} k^2 \lambda_D^2\right)$$

$$\times \exp\left[- T_o/2ak^2\lambda_D^2 \, T(x)\right] , \qquad (18)$$

where we have approximated $\exp(-3/2) \approx 1/4.5$; also asymptotic expansions in powers of the small parameters ε and $k^2\lambda_D^2$ have been used. At the plasma center $T(0) = T_o$ and the exponential in (18) becomes equal to the exponential in Landau's damping coefficient given in (8), because λ_D in (18) as in all the rest of the paper designates the Debye length at the plasma center, $\lambda_D \equiv \lambda_D(0)$. The transport equation (16) is a first-order linear differential equation whose exact solution is

$$E(x,\underline{k}) = \int_o^{\mu(-L,x)} e^{-\mu} \, T(z) d\mu ,$$

$$\mu(z,x) \equiv \int_z^x \lambda(x')dx' . \qquad (19)$$

The total energy loss per unit volume of the plasma is obtained by integrating over all the waves

$$A(x) = \frac{1}{(2\pi)^2} \int d^2\underline{k} |v_x| \left|\frac{dE}{dx}\right| = \frac{1}{(2\pi)^2} \int d^2\underline{k} |v_x| |\lambda(x)| \left[T(x) - E(x,\underline{k})\right]$$

$$= \frac{1}{(2\pi)^2} \int d^2\underline{k} \; 2\gamma_L(x) \left[T(x) - E(x,\underline{k})\right] . \qquad (20)$$

We now calculate the rate of energy loss at the plasma center A(0); this requires the evaluation of $T(0) - E(0,\underline{k})$ in the integrand of (20). It is noted that from (19)

$$\mu_{max} \equiv \mu(-L,o) = \int_{-L}^{o} \lambda(x')dx' = \int_{o}^{L} \lambda(x')dx' \approx$$

$$\lambda(0)\int_{o}^{L} \exp(-x^2/2ak^2\lambda_D^2L^2)\ dx \approx \lambda(0)\int_{o}^{\infty} \exp(-x^2/2ak^2\lambda_D^2L^2)dx$$

$$= \lambda(0)(\pi/2)^{1/2}\ a^{1/2}\ k\lambda_D L\ . \qquad (21)$$

In (21), we have expanded $\lambda(x)$ (see Eq. (18)) near the plasma center by setting explicitly $T_o/T(x) = T_o/T_o(1-x^2/L^2) \sim 1 + x^2/L^2$; this is justified because $T(L) = 0$, and (18) shows that wave absorption becomes vanishingly small near the plasma boundary. Putting $\mu_{max} = \mu(-L,o)$ and $T(z) = T_o(1 - z^2/L^2)$ in (19) and noting that for $\mu_{max} >> 1$, we can approximate $\sinh \mu_{max} \sim \cosh \mu_{max}$, Eq. (19) gives[3]

$$T(0) - E(0,\underline{k}) = \frac{T_o}{L^2}\ \frac{\int_{o}^{\mu_{max}} z^2 \cosh(\mu - \mu_{max})d\mu}{\sinh \mu_{max}}\ . \qquad (22)$$

Substituting now (21) and (22) in (20), we get

$$A(0) \simeq \frac{1}{(2\pi)^2}\iint k\,d\theta\,dk\,\frac{\omega_p k_x k_y}{a^{1/2}k^3}\,(1-\varepsilon\cos^2\theta+\frac{9}{2}k^2\lambda_D^2)\,(\frac{2}{\pi})^{1/2}$$

$$\times\frac{1}{a^{1/2}k\lambda_D L}\,\mu_{max}\,\frac{T_o}{L^2}\,\frac{\int_o^{\mu_{max}} z^2\cosh(\mu-\mu_{max})d\mu}{\sinh\mu_{max}}\,. \qquad (23)$$

The integrations in (23) are carried out as follows. First, the last integral in (23) is integrated by parts, noting that $\mu(z,o)$ appearing in the integrand is obtained from (19) as $\mu(z,o) = \mathrm{erf}(z/2^{1/2}\,a^{1/2}\,k\lambda_D L)\mu_{max}$; the result of the integration by parts is

$$\int_o^{\mu_{max}} z^2\cosh(\mu-\mu_{max})d\mu \approx 4ak^2\lambda_D^2L^2\int_o^{\infty} v\,dv\,\sinh\mu_{max}(1-\mathrm{erf}\,v). \qquad (24)$$

Now we change variables in (23) from k to μ_{max} ; using $\lambda(o)$ as given by (18) into (21), one gets

$$\mu_{max} = \frac{\pi}{2}\,\frac{1}{4.5}\,\frac{L}{\lambda_D}\,\frac{1}{k_x\lambda_D}\,\frac{1+\varepsilon\cos^2\theta-(9/2)k^2\lambda_D^2}{a}\,\exp(-1/2ak^2\lambda_D^2)$$

$$\equiv C\,\exp(-1/2ak^2\lambda_D^2)\ ; \qquad (25)$$

now if the dependence of C on k is neglected with respect to the stronger dependence given by the exponential, we get

$$k\,dk \approx k^4\lambda_D^2\,a\,d\mu_{max}/\mu_{max}\ . \qquad (26)$$

Substituting (24-26) into (23), we get

$$A(0)=\frac{2^{1/2}}{\pi^{5/2}}\frac{\omega_p T_o}{L\lambda_D}\iint d\theta\ d\mu_{max}|\sin\theta\ \cos\theta|\,(1-\varepsilon\cos^2\theta+\frac{9}{2}k^2\lambda_D^2)$$

$$\times\ a(k\lambda_D)^4\ \frac{\int_o^\infty v\ dv\ \sinh\mu_{max}\ (1-\text{erf}\ v)}{\sinh\mu_{max}}\ . \qquad (27)$$

Approximating further the expression in (25) by

$$\mu_{max}\approx(L/\lambda_D)\ \exp(-1/2ak^2\lambda_D^2)\ , \qquad (28)$$

we get

$$k\lambda_D\approx(2a\ \ell n\ L/\lambda_D\ \mu_{max})^{-1/2}\ . \qquad (29)$$

As Rosenbluth and Liu pointed out,[3] it is clear that the most important wavelengths contributing to the energy transport are those whose absorption mean free path is of the order of the length of the system, i.e., $\ell_{mfp}(0)=1/\lambda(0)\approx L$. Using (21), it can be seen that these wavelengths are those corresponding to $\mu_{max}\approx 1$. Therefore, $k\lambda_D$ in (27) is substituted by its expression (29) with $\mu_{max}\approx 1$, and we get

$$A(0)=\frac{2^{1/2}}{\pi^{5/2}}\frac{\omega_p T_o}{L\lambda_D}\iint d\theta\ d\mu_{max}|\sin\theta\ \cos\theta|\left[(1-\varepsilon\cos^2\theta)\ \frac{1}{4a\ \ell n^2(L/\lambda_D)}\right.$$

$$\left.+\frac{9}{2}\frac{1}{8a^2\ell n^3(L/\lambda_D)}\right]\frac{\int_o^\infty v\ dv\ \sinh\mu_{max}(1-\text{erf}\ v)}{\sinh\mu_{max}}\ . \qquad (30)$$

Using the definition of $\underline{a}$ given by (17), we get the following asymptotic expansions

$$(1-\varepsilon\cos^2\theta)/a=(1-\varepsilon\cos^2\theta)/(1+\varepsilon\sin^2\theta)\sim(1-\varepsilon\cos^2\theta)(1-\varepsilon\sin^2\theta)\sim 1-\varepsilon,$$

$$1/a^2 = 1/(1+\varepsilon\sin^2\theta)^2 \sim 1 - 2\varepsilon\sin^2\theta \qquad (31)$$

After substituting (31) into (30), the angle integrals are done by elementary means. It is now noted that the integral with respect to μ_{max} is of the form $\int_o^\infty (\sinh px/\sinh x)dx$ and is known in closed form.[10] The remaining v-integral was obtained numerically in Ref. 3, so that

$$\int_o^\infty d\mu_{max}\,\frac{\int_o^\infty v\,dv\,\sinh\mu_{max}(1-\operatorname{erf} v)}{\sinh\mu_{max}} = 8.25\times 10^{-1}\,. \qquad (32)$$

Finally, the rate of energy loss at the plasma center is given by:

$$A(0) = 3.34\times 10^{-2}\,\frac{\omega_p T_o}{L\lambda_D}\left(1-\frac{\omega_p^2}{\omega_c^2}\right)\frac{1}{\ell n^2(L/\lambda_D)}$$

$$\times\left[1 + 2.25\,\ell n^{-1}(L/\lambda_D) + O(\ell n^{-2}L/\lambda_D)\right]. \qquad (33)$$

The term $O(\ell n^{-2}L/\lambda_D)$ in (33) would be obtained using a third-order dispersion relation instead of (8). The result (33) gives

the first two terms of a series which is asymptotic in the limit $L/\lambda_D \to \infty$. Rosenbluth and Liu's treatment gives essentially the first term of (33) when $\omega_c \to \infty$ also. The importance of the second-order term in (33) is that it provides an inner consistency check of the validity of the asymptotic theory. Thus, for $L/\lambda_D = 8$, the series (33) does not converge well, because its second term is as large as the first term (see Table I); the reason is that the most important wavelength for the energy transport given by (29) with $\mu_{max} \approx 1$, $a \approx 1$, is $k\lambda_D \approx 0.5$, for which the long wavelength dispersion relation used [see (8)] is not quite correct. As shown clearly in Fig. 3 of Ref. 6, the long wavelength dispersion relation is reasonably correct for $k\lambda_D < 0.5$. Whenever $k\lambda_D$ as determined by (29) approaches 0.5 , the asymptotic theory starts to break down as is indicated plainly by the data in Table I. These data show quite clearly that, for a convincing verification of the theory, the numerical simulation of wave energy transport requires a fairly large computer plasma (where $L/\lambda_D = 16$ at least). Furthermore, the second-order term in (33), which originates in the second-order dispersion relation (8), provides a substantial correction to the first-order treatment,[3] even for the large sizes shown in Table I; this result is consistent with the fact that the second-order dispersion relation (8) is substantially more accurate than the first-order one, even for quite long wavelengths.[8] It should also be noticed that wave energy transport increases slowly with the magnetic field, and in the

limit $\omega_c \to \infty$ it becomes independent of its magnitude, in agreement with the first order treatment.[3]

Finally, it should be noticed that only some trivial differences in the k- and θ-dependence of the integrand in (23)distinguish our two-dimensional treatment from the three-dimensional treatment of Ref. 3.

B. Weak Magnetic Field Limit

Here we give the calculation of the energy transport valid for $\omega_c \leq \omega_p$. This calculation is similar to that given in the previous section. The absorption probability is determined as before from the corresponding dispersion relation (15), $\lambda(x)=2\gamma_L/v_x$. The group velocity is

$$v_x = \frac{d(\mathrm{Re}\omega)}{dk_x} = \omega_p \frac{k_x k_y^2}{k^4} (\varepsilon + 3k_y^2\lambda_D^2),$$

$$\varepsilon \equiv \omega_c^2/\omega_p^2. \tag{34}$$

The absorption probability is then

$$\lambda(x) = \frac{2\gamma_L}{v_x} = (\pi/2)^{\frac{1}{2}} \frac{1}{n!} \frac{1}{2^n} \frac{\sin^{2n-1}\theta \ (\omega_p/\omega_c)^{2n}}{\lambda_D \cos^3\theta \ (\varepsilon+3k_y^2\lambda_D^2)}$$

$$\times (k\lambda_D)^{2n-2} \ (1-x^2/L^2)^{n-1} \equiv \lambda(0) \ (1-x^2/L^2)^{n-1} \tag{35}$$

where we recall that n is the lowest integer closest to the ratio ω_p/ω_c. Because of the simple algebraic dependence of the absorption probability on the distance, the treatment is now

much simpler than for the strong magnetic field case. In particular expanding the temperature profile in (35) about the plasma center and integrating term by term, one gets

$$\mu_{max} = \mu(0,L) = \int_0^L \lambda(x')dx' \simeq \left[1-\frac{n-1}{3} + \frac{(n-1)(n-2)}{10} \ldots\right] \lambda(0)L$$

$$\equiv c\lambda(0)L$$

$$\mu(0,z) = \int_0^z \lambda(x')\, dx' = c\lambda(0)z. \tag{36}$$

It should be noticed that the formal solution of the transport equation (16) is given exactly by (19) for any given $\lambda(x)$. Using (19) and (36), we get quite simply

$$T(0) - E(0,\underline{k}) = \frac{T_0}{L^2} \frac{1}{c^2\lambda^2(0)} \int_0^{\mu_{max}} \mu^2 \exp(-\mu)\, d\mu$$

$$\simeq \frac{0.16}{c^2\,\lambda(0)} \frac{T_0}{L^2}\,, \tag{37}$$

where the integral has been evaluated taking $\mu_{max}=1$; this means that for purposes of integration the important wavelengths are those with an absorption mean free path of the order of the length of the system, i.e., $l_{mfp}=1/\lambda(0)\simeq L$ (see (36)). The energy flux at the plasma center is now given by (see Eqs. (20) and (23)):

$$A(0) = \frac{1}{(2\pi)^2}\iint k\, d\theta\, dk\, \frac{\omega_p k_x k_y^2}{k^4}\,(\varepsilon+3k_y^2\lambda_D^2)$$

$$\times\, \lambda(0)\,\frac{0.16}{c^2\lambda^2(0)}\,\frac{T_0}{L^2}\,. \qquad (38)$$

Using again the basic simplification of taking $\mu_{max}=c\lambda(0)L=1$ in the integrand of (38), the remaining k- and θ-integrations are done by elementary means. We obtain finally

$$A(0) = \frac{3.2\times10^{-3}}{c}\,\frac{\omega_p T_0}{L\lambda_D}\,(1 + 1.67\,\omega_c^2/\omega_p^2), \qquad (39)$$

where c is the constant close to unity defined by (36) in terms of the lowest integer n closest to the ratio ω_p/ω_c. The second term in (39) is almost negligible relative to the first term; this latter depends only weakly on the magnetic field magnitude through the constant $c\lesssim 1$. Therefore, for a plasma in a weak magnetic field, wave transport is almost independent of its magnitude.

Lastly, the calculation of the energy flux for the limiting case $\omega_p\doteq\omega_c$ is even easier than for the limit $\omega_p>\omega_c$. The details of the calculation are given in Appendix A, and the result is

$$A(0) = 4.6\,\times10^{-3}\,\frac{\omega_p T_0}{L\lambda_D}\,. \qquad (40)$$

Because wave energy transport is almost independent of the

magnetic field magnitude, in this region this process is not as important as classical collisional transport, because this latter varies as $1/B^2$; this is confirmed by our simulation results to be discussed below.

IV. COMPUTER SIMULATIONS

In this section, we give the results of the simulations of wave energy transport, and compare them with the theoretical results obtained in Section III. For strong magnetic fields, the computations verify the theoretical prediction that energy transport by plasma waves increases slowly with the magnetic field, and that in the limit of large field magnitudes wave transport dominates classical collisional transport. For weak fields, the simulation shows that collisional transport is more important than wave transport, also in agreement with the theory.

A. The Simulation Model

As shown in Section III, waves propagating obliquely to the magnetic field contribute to the energy transport, while those traveling in the perpendicular direction are not Landau damped (see Ref. 4, p. 226), and therefore,

cannot be absorbed. In order to simulate energy transport by plasma waves, we require therefore that their $\underline{k}$-vectors have all possible directions relative to the magnetic field. This requirement is met by the 2 1/2-dimensional (two positions and three velocity components) electrostatic particle model shown in Fig. 1.[2] The magnetic field is in the y-direction and the initial electron temperature profile was chosen to be

$$T(x,0) = T_b[1 + 3 \sin (\pi x/2L)] , \tag{41}$$

which is parabolic at the plasma center, as assumed in the theory, and is also periodic in the x-direction with a period 2L equal to the plasma size. We assume that the plasma is periodic, and because it is also symmetric with respect to the x = L plane, the periodic boundary conditions are equivalent to reflective boundary conditions with respect to the relaxation of the temperature profile. As mentioned before, the ions are assumed to form an immobile uniform background.

A very significant advantage of the model shown in Fig. 1 is that it can completely eliminate the large energy transfer due to electron convective cells,[2] because the $c\,\underline{E} \times \underline{B}/B^2$ drift velocity of the electrons is always in the z-direction, and therefore it does not contribute to the relaxation of the temperature profile in the x-direction. On the other hand, because of the discreteness of the simulation model, it is not possible

to eliminate the energy transfer due to binary collisions completely. However, as we show below, there is an unambiguous way of separating the energy transfer by plasma waves from the collisional transfer. This is because energy transfer by plasma waves is due to their Landau damping along the magnetic field, and as a result only the parallel component of the temperature decreases. The relaxation of the perpendicular component of the temperature results from collisional diffusion, because waves are not damped in the perpendicular direction (see Ref. 4, p. 226). There is of course collisional relaxation between the parallel and perpendicular temperatures.[11] The relaxation time for this process is given essentially by the 90° collision time and is independent of the magnetic field strength. Because the cross-field diffusion distance is smaller than the gyroradius, the characteristic time for collisional relaxation between the parallel and perpendicular components of the temperature is longer than the cross-field diffusion time. This is confirmed by the simulation results to be discussed below.

It should be noted here that using a particle code, the perpendicular and parallel components of the average temperature of a particle can be output very simply, as they are defined by

$$T_{\perp} = (1/3)\ m\ \ (\langle v_x^2 \rangle + \langle v_z^2 \rangle) \equiv (1/3)\ m\ \ \langle v_{\perp}^2 \rangle\ ,$$

$$T_{\parallel} = (1/3)\ m\ \ \langle v_y^2 \rangle \equiv (1/3)\ m\ \ \langle v_{\parallel}^2 \rangle \qquad (42)$$

where m is the electron mass, and $< v_\perp^2 >$ and $< v_\parallel^2 >$ are averages of the square of the velocities in the perpendicular and parallel directions.

For a sufficiently short time in which the relaxation of the initial temperature is small, we may assume that

$$T_\perp(t)/T_\perp(0) = 1 - \nu_c t \equiv 1 - \nu_\perp t \ ,$$

$$T_\parallel(t)/T_\parallel(0) = 1 - (\nu_c + \nu_w)t \equiv 1 - \nu_\parallel t \ , \qquad (43)$$

where ν_c and ν_w are the relaxation rates due to collisional and wave transport respectively. Collisions tend to relax the temperature equally in the parallel and perpendicular directions, while wave transport leads to a decrease of the temperature in the parallel direction only. The simulation results below show that the basic assumption (43) is satisfied well. Initially the electron velocity distribution is an isotropic Maxwellian distribution, i.e., $T_\perp(0) = 2T_\parallel(0)$, because there are two degrees of freedom in the transverse direction [see Eq. (42)]; noting this, the relaxation of the total electron temperature can be obtained from (43) as:

$$T(t)/T(0) \equiv [T_\perp(t) + T_\parallel(t)]/3T_\parallel(0)$$

$$= 1 - (\nu_c + \nu_w/3)t \equiv 1 - \nu t \ . \qquad (44)$$

We must now relate the electron temperature profile, which is given by the simulation as a function of time, with the wave energy flux obtained theoretically in Section III

[i.e., Eqs. (33), (39), and (40)]. The set of time-dependent equations coupling the wave energy with the electron temperature may be written as follows:

$$\frac{1}{(2\pi)^2}\int d^2\,\underline{k}\left[\frac{\partial E(t,x,\underline{k})}{\partial t} + v_x\,\frac{\partial E}{\partial x} + 2\gamma_L E\right] = \frac{1}{(2\pi)^2}\int d^2\,\underline{k}\;2\gamma_L T\ , \qquad (45)$$

$$\frac{3}{2}\,\frac{\partial nT(x,t)}{\partial t} = \frac{\partial}{\partial x}\,D\,\frac{\partial nT}{\partial x} + \frac{1}{(2\pi)^2}\int d^2\,\underline{k}\;2\gamma_L(E - T)\ , \qquad (46)$$

where D is the classical collisional diffusion coefficient,[2] n is the electron density, and the other symbols have been defined before. Equation (45) is the wave energy conservation equation; it expresses the fact that the rate of change of wave energy per unit volume is due to the divergence of the energy flux $\underline{v}_x E$, to the wave absorption by Landau damping and to the spontaneous Cerenkov emission of the waves.[12] Equation (46) is the balance equation for the heat density; it states that its rate of change is due to losses by collisional heat transfer and wave transport. We have neglected convective heat transfer and generation of heat due to viscosity[13] because for the present simulation model (Fig. 1) the drift velocity is primarily in the z-direction. This assumption is verified by the simulation results to be discussed below. Adding Eqs. (45) and (46), and then integrating over the whole plasma volume, we obtain

$$\frac{\partial}{\partial t}\int_V\left[\frac{3}{2}\,nT + \frac{1}{(2\pi)^2}\int E\,d^2\underline{k}\right] d^2\underline{x} = 0\ , \qquad (47)$$

because the divergence terms in both equations vanish when integrating over the whole plasma. Equation (47) expresses then the conservation of the total energy of the plasma.

The electron temperature, given by Eqs. (45) and (46) together with the initial condition (41), is expanded as follows:

$$T(x,t) \approx \sum_{j=-N}^{N} C_j(t) \exp(ij\pi x/L) \ , \qquad (48)$$

where the coefficients $C_j(t)$ are given directly by the particle simulation code. The decay of the Fourier coefficient gives a much more reliable and smooth measurement of the relaxation rate than the decay of the temperature measured locally at the center, because the Fourier coefficient is obtained by averaging the temperature profile over many spatial points. The space-independent component does not change with time because it gives rise to a uniform system for which the steady-state solution [see Eq. (16)] is $E_o = T_o$ and (46) gives $dC_o/dt = 0$. Because of the initial condition (41), we expect that the amplitude of the first space-dependent Fourier mode is much larger than that of the higher modes, i.e.,

$$|C_1(t)| >> |C_j(t)| \ , \quad j \geq 2 \qquad (49)$$

which is indeed confirmed by the numerical results. Therefore, using Eqs. (41), (46), (48), and (49), and noting that for the initial condition (41) $C_1(0) = -0.64\ T_b$ we get for the rate of change of the temperature at the plasma center:

$$\frac{3}{2}\, n\, \frac{\partial T(L,t)}{\partial t} = -3n\left[\left(\frac{dC_1}{dt}\right)_c + \left(\frac{dC_1}{dt}\right)_w\right]$$

$$= \left[\frac{\partial}{\partial x}\, D\, \frac{\partial nT}{\partial x}\right]_{x=L} + \left[\frac{1}{(2\pi)^2}\int d^2\underline{k}\; 2\gamma_L(E - T)\right]_{x=L}, \qquad (50)$$

after having separated the amount of the temperature decay due to the wave transport from that due to classical collisional transport. During a sufficiently short time in which the temperature decay is quite small, the wave energy does not change much either; therefore, the time-dependent term in (45) can be neglected in a first approximation, and the energy flux at the plasma center due to wave transport in (50) is approximated by the flux [see Eq. (20)] obtained from the solution of the steady-state equation (16), i.e., by Eqs. (33), (39), and (40). The agreement between theoretical and numerical results shown below is the most convincing proof of the validity of this assumption. (Note that, Fig. 1, for notational convenience the center of the computer plasma is at $x = L$, which corresponds to $x = 0$ for the theoretical plasma.) Therefore, Eq. (50) gives

$$\left(\frac{d|C_1|}{dt}\right)_w \approx -\frac{A(0)}{3n}\,. \qquad (51)$$

We now divide both sides of (51) by $|C_1(0)|$, and it is noted that from (41), $|C_1(0)| = 0.64\, T_b = (0.64/4)T(L,0) = 0.16\, T_o$, where T_o is the notation used in the theory for the temperature at the plasma center; as in the simulation the time is in units

of ω_p^{-1} , we finally obtain the rate of relaxation of the total plasma temperature [see also (43) and (44)]:

$$\frac{1}{C_1(0)}\left[\left(\frac{dC_1}{dt}\right)_c + \left(\frac{dC_1}{dt}\right)_w\right] = -\nu_c - \frac{\nu_w}{3} = -\nu_c - 2.08\,\frac{A(0)}{n\omega_p T_o} . \quad (52)$$

The relative rates of the total temperature relaxation due to wave transport and collisional transport, $\nu_w/3$ and ν_c , are quantities which are measured directly in the simulation. The rate of temperature decay due to wave transport will be compared below with the theoretical energy flux A(0) given by Eqs. (33), (39), and (40).

B. Numerical Results

The initial conditions used with the particle code are similar in many respects to those described before in considerable detail.[2] As we are interested in a thermal plasma with all modes of the system excited, no quiet start was used. The guiding centers were uniformly loaded on the (x,y)-plane, and the initial velocity distribution was an isotropic local Maxwellian to ensure an accurate thermal spectrum. The thermal velocities of the Maxwellian electrons were chosen so as to give the temperature distribution (41). The electrostatic energy per mode of wavenumber k in a thermal equilibrium plasma with a uniform temperature distribution is[2,14]

$$(\delta E^2)_k/8\pi = (KT/2)\left[1 + k^2\lambda_D^2 \exp(k^2a^2)\right]^{-1} , \qquad (53)$$

where δE is the electric field amplitude, and a is the width of the finite size gaussian cloud,[14] which was taken equal to the grid size in all the simulations. Because the Poisson equation is solved in $\underline{k}$-space replacing $\nabla^2\phi$ by $-k^2\phi$, there are very small grid effects on the thermal spectrum even for large k modes; this is verified by the agreement between the simulation results and Eq. (53) (see Figs. 2 and 3). Equation (53) has been used with T and λ_D^2 defined as rough averages of the actual temperature profile and Debye length; specifically, for the temperature profile (41) we took $\bar{T} \approx 2.5$ and $\bar{\lambda}_D^2 \approx \lambda_D^2(0)\bar{T} = 2.5$. The computed electrostatic energy in each mode was compared with the theoretical fluctuation spectrum given by (53). The results obtained in two typical computations are shown in Figs. 2 and 3. Although not nearly as good as the agreement found before for a plasma with a uniform temperature profile (see Fig. 2 of Ref. 2), there is unquestionably a semiquantitative agreement between the computed and theoretical thermal equilibrium spectrun, making us confident that our computer plasma is reasonably close to local thermal equilibrium.

In Fig. 4, we show the results of the simulation for the case run with the strongest magnetic field, $\omega_p/\omega_c = 1/4$. As discussed in the previous subsection, the relaxation of the temperature at the plasma center, T , is given by the decay of the first spatially-dependent Fourier mode of the temperature

profile [see Eqs. (48-52)]. Furthermore, the particle code gives separately the parallel and perpendicular temperature components, $T_{\parallel}$ and $T_{\perp}$ [see Eqs. (42-44)]. The basic assumption (43) is confirmed very satisfactorily by the results shown in Fig. 4. For this case with a very strong magnetic field, the decay of $T_{\parallel}$ is due mostly to wave transport, and approaches its maximum limiting value for $\omega_p/\omega_c \to 0$ [see Eqs. (33) and (52)]. On the other hand, the decay of $T_{\perp}$ is entirely due to collisions and is significantly smaller than the decay due to wave transport, as expected. Using Eq. (43), we get $\nu_c = \nu_{\perp} = 2.6 \times 10^{-6}$, and $\nu_w = \nu_{\parallel} - \nu_{\perp} = 4.74 \times 10^{-5}$; the total temperature decay rate is now obtained from (44), $\nu = \nu_c + \nu_w/3 = 1.84 \times 10^{-5}$, and this checks well the experimental value (Fig. 4), $\nu = 1.9 \times 10^{-5}$, showing that the slopes of the straight lines drawn through the computed points are consistent with Eqs. (43) and (44). One should note that because the average gyroradius is about one half of the particle size, the particles do not collide with each other within the gyroradius. This explains why the collisional relaxation is so small in this simulation. It should also be noticed that collisional transport will vanish in the limit of very large magnetic fields and, Eqs. (43) and (44), $\nu_{\perp} = \nu_c \to 0$, $\nu_{\parallel} = \nu_c + \nu_w \to (\nu_w)_{max}$, and $\nu/\nu_{\parallel} \to \nu/(\nu_{\parallel})_{max} \to 1/3$; the results in Fig. 2 give $\nu/\nu_{\parallel} = 0.38$ showing that this limit is being approached. Thus, for very strong magnetic fields where collisional transfer is negligible, the effect of wave energy transport is to produce a significant anisotropy in the local velocity distribution, because only the parallel component of the temperature decays.

In Table II, the theoretical results obtained for the strong magnetic field case, Eqs. (33) and (52), are compared with the simulation results. Because the computer plasma size used, $L/\lambda_D = 16$, is not as large as might have been desired for the strong asymptotic convergence of the result (33) (see Table I), the agreement between the theoretical and the numerical results might be considered quite satisfactory.

All computations in this paper were done with an IBM 360/91 computing system. Depending on the magnetic field strength, the computing time required for each case varied from 5 to 12 hrs. The total physical time followed was almost $1000\ \omega_p^{-1}$, and the time step used was $\Delta t = 0.1 - 0.2\ \omega_p^{-1}$. The total number of particles used was 65,536 and the grid was 64 x 64 . This is the reason for not having computed with even larger plasma sizes.

In Fig. 5, we give the results of a simulation where $\omega_p/\omega_c = 1/2$, this is a weaker magnetic field than that in Fig. 4. As expected, collisional transport becomes more important, as indicated by the significant increase in the decay rate of the perpendicular component of the temperature with respect to the case in Fig. 4. Using only the numerical values of $\nu_{\parallel}$ and $\nu_{\perp}$ and Eq. (43), one gets $\nu_c = \nu_{\perp} = 1.6 \times 10^{-5}$, and $\nu_w = \nu_{\parallel} - \nu_{\perp} = 3.3 \times 10^{-5}$; therefore, from (44) the total temperature decay rate is $\nu = \nu_c + \nu_w/3 = 2.7 \times 10^{-5}$, which agrees well with the experimental value shown in Fig. 5. The relaxation of the parallel component of the temperature due to wave transport is about twice as high as that due to

collisions, i.e., $\nu_w \approx 2\nu_c$. However, the decay of the total temperature due to wave transport is only one third of the wave decay rate of the parallel component [see (44)]. As a consequence, for this simulation the contributions to the total temperature decay rate from collisional and wave transport are almost the same (see Table II). The agreement of the theoretical results, Eqs. (33) and (52), with the numerical results for $\omega_p/\omega_c = 1/4$ and $\omega_p/\omega_c = 1/2$ shown in Table II is a striking confirmation of the fact that the dependence of wave transport on the magnetic field is as predicted by the theory.

In Fig. 6, we show the results of the simulation for the case with $\omega_p/\omega_c = 1$. The most obvious difference relative to Figs. 4 and 5 is that the relaxation rates of the total, parallel and perpendicular temperatures are now approaching each other, indicating clearly that collisional transport is now dominant and that the anisotropy in the temperature decay due to wave transport is becoming quite small. Using (43) and the numerical values of $\nu_{\parallel}$ and $\nu_{\perp}$, one gets $\nu_c = \nu_{\perp} = 4.7 \times 10^{-5}$, and $\nu_w = \nu_{\parallel} - \nu_{\perp} = 3.3 \times 10^{-5}$; thus, the total temperature decay rate is from Eq. (41) $\nu = \nu_c + \nu_w/3 = 5.1 \times 10^{-5}$, which agrees with the numerical result in Fig. 6. Because only one third of the wave decay rate contributes to the total decay rate, this latter is now mostly due to collisional transport; more precisely, Table II shows that the total decay rate due to collisional transport is now over 12 times higher than that due to wave transport. It is worth noting that for the stronger fields the collisional relaxation rate scales approximately as B^{-2} (see Table II), in rough agreement with the classical

theory. It should be noticed that the present model is not quite appropiate for the study of collisional diffusion.[2] The agreement between theory and simulation shown in Table II is not as satisfactory as for the previous two cases, although the theoretical wave decay rate shows the correct qualitative dependence on the magnetic field magnitude.

In Fig. 7,we give the results of the simulation for the only weak magnetic field case run, ω_p/ω_c =2.5. The decay rates are now mostly due to collisions, although one can notice that the parallel decay rate is still higher than the perpendicular decay rate, indicating that wave transport effects are still noticeable. The precise data obtained from the numerical results and Eqs. (43) and (44) are given in Table II. Figure 7 indicates clearly the approach to the limit of very small magnetic fields, when energy transport would become entirely dominated by collisions and the decay rates of the total,parallel and perpendicular temperatures would become equal, the anisotropy due to wave transport being finally negligible. Table II shows that the theoretical result obtained for the weak magnetic field case, Eqs. (39) and (52), is in fair agreement with the simulation, even though the theoretical result is based on the simplification $\omega_p/\omega_c \simeq 2$. More significant is the fact that the theoretical results for the two weak magnetic field cases, $\omega_p/\omega_c = 1$ and 2.5, show the correct qualitative dependence on the magnetic field magnitude as given by the simulations.

Both the theoretical and numerical results in Table II establish that wave transport increases slowly with the magnetic field, and that in the range shown,wave transport is of the same order of magnitude. Indeed, one does not need very strong magnetic fields for wave transport to be a significant effect.

V. CONCLUSION

It has been shown that cross-field energy transport by plasma waves is a slowly increasing function of the magnetic field. For strong magnetic fields, $\omega_c > \omega_p$, its magnitude remains of the same order while approaching its maximum limiting value for $\omega_c \to \infty$. Because collisional transport decreases markedly as the magnetic field increases, when $\omega_c > \omega_p$ wave transport can be more important than collisional transport, even for the small plasmas ($L/\lambda_D = 16$) used in our simulations. As Rosenbluth and Liu have pointed out, when the size of the system increases, wave transport becomes even more predominant.

It should be noted that in the present simulation model, heat conduction due to low frequency ion waves[2] has been deliberately eliminated. However, in a real plasma in a strong magnetic field this process may be more important than classical or wave transport. As opposed to the case of collisional transport, the relaxation of the temperature due to wave transport leads to an anisotropic velocity distribution in a strong magnetic field, when the relaxation time of the collisional process that results in an isotropic distribution is long.

It is expected that any mechanisms which modify the amplitudes of the waves or their dispersion properties can change the wave transport process significantly. Many of the laboratory plasmas are subject to instabilities which will enhance wave transport as well as convective transport. It is also

possible that radio frequency plasma heating can significantly enhance the wave transport process.

Near the center of the plasma column of present tokamak devices, ω_c is typically a few times larger than ω_p ; therefore, near the boundary $\omega_c >> \omega_p$, and anomalous transport processes such as those due to convective cells and waves are dominant over collisional transport.

Finally, it is perhaps worthwhile to emphasize the importance of simulation methods to investigate problems such as heat transfer due to waves. It would be extremely difficult to study this phenomenon in laboratory experiments, because many physical effects occur simultaneously and they cannot be separated from each other. The agreement between theory and numerical results confirms the validity of the present simulation model to study wave transport.

ACKNOWLEDGMENTS

One of the authors (J. C.) expresses his deep appreciation to Drs. Horace Flatt (IBM) and Melvin Gottlieb (PPPL) for having given him the opportunity to spend a year at PPPL. The authors are grateful to Prof. J. M. Dawson who was involved in the initial stages of the work. The help provided in the computations by H. Fallon, R. F. Kluge, and Y. C. Sun is also gratefully acknowledged.

This work was supported by USAEC under Contract AT(11-1)-3073.

APPENDIX A

Here we obtain the wave energy flux for the special case $\omega_p=\omega_c$, given in Eq. (40) of the text. The Landau damping coefficient is given by Eq. (15) of the text with n=1. However, the frequency is not given by Eq. (15) and must be obtained by the following special treatment. Expanding the w-function in Eq. (4) for large values of the argument and keeping only algebraic terms (as we are solving for the frequency only), one gets to first order

$$K^2 \left(-\frac{1}{2z^2}\right) + \ldots + K^2 \sin^2\theta \frac{z_p^2}{z_p^2 - z^2} = 0, \qquad \text{(A1)}$$

having used $z_c=z_p$. Eq. (A1) after a little manipulation is reduced exactly to a biquadratic equation whose solution is $z = z_p(1+\sin\theta)^{\frac{1}{2}}$. In physical variables:

$$\omega \sim \omega_p(1+\sin\theta)^{\frac{1}{2}} - i(\pi/8)^{\frac{1}{2}} \frac{\omega_p}{k^3\lambda_D^3 \cos\theta} (1/2)\, k^2\lambda_D^2 \sin^2\theta. \qquad \text{(A2)}$$

The treatment is now the same as that given in the main text for the weak magnetic field case. So

$$\lambda(x) = \frac{2\gamma_L}{v_x} = (\pi/2)^{\frac{1}{2}} \frac{\sin^2\theta}{\cos^3\theta} \frac{1}{\lambda_D} \frac{1}{(1-x^2/L^2)^{\frac{1}{2}}}$$

$$\equiv \lambda(0) \frac{1}{(1-x^2/L^2)^{\frac{1}{2}}}. \qquad \text{(A3)}$$

Also,we get

$$\mu_{max} = 1.17\ \lambda(0)L, \qquad \mu = 1.17\ \lambda(0)z, \tag{A4}$$

and further,

$$T(0) - E(0,\underline{k}) = \frac{0.12}{\lambda^2(0)}\ \frac{T_0}{L^2}\ . \tag{A5}$$

Substituting (A5) into the expression corresponding to (38) of the text, and carrying out the k- and θ-integrations, we get the desired result, Eq. (40) of the text.

Table I. The convergence of the series (33) as a function of the plasma size.

L/λ_D	$k\lambda_D = {}^a (2\ell n\ L/\lambda_D)^{-1/2}$	Second-order term[b] $2.25\ \ell n^{-1}\ L/\lambda_D$
4	0.6	1.62
8	0.49	1.08
16	0.42	0.81
10^2	0.33	0.49
10^3	0.27	0.33
10^4	0.23	0.24
10^5	0.21	0.19

[a]These are the wavelengths that for each size contribute most to the energy transport, see Eq. (29).

[b]Note that the relative magnitude of the first-order term is unity.

Table II. Total temperature decay at the plasma center due to wave transport and collisional transport as a function of the magnetic field.

	Temp. decay by plasma waves, $\nu_w/3$			Collisional temp. decay, ν_c	Wave transport vs. Collis. transport $(\nu_w/3)/\nu_c$
ω_p/ω_c	Theory[a]	Simulation	Th./Sim.	Simulation	
1/4	1.5×10^{-5}	1.6×10^{-5}	0.94	0.26×10^{-5}	6.1
1/2	1.2×10^{-5}	1.1×10^{-5}	1.09	1.6×10^{-5}	0.7
1	0.9×10^{-5}	0.4×10^{-5}	2.25	4.7×10^{-5}	0.08
2.5	1.2×10^{-5}	1.0×10^{-5}	1.20	1.0×10^{-4}	0.1

[a]For $\omega_p/\omega_c < 1$, the theoretical values are obtained from Eqs. (33) and (52), for $\omega_p/\omega_c > 1$ from (39) and (52), and when $\omega_p/\omega_c = 1$ from (40) and (52); the plasma half width is $L = 32$, the Debye length at the plasma center is $\lambda_D = 2$, so that $L/\lambda_D = 16$ (see Table I), and finally the electron density is $n = 256 \times 256/64 \times 64 = 16$.

REFERENCES

*Permanent address: IBM Scientific Center, Palo Alto, California 94304.

[1]J. B. Taylor and B. McNamara, Phys. Fluids 14, 1492 (1971).

[2]H. Okuda and J. M. Dawson, Phys. Fluids 16, 408 (1973); also R. F. Kluge, H. Okuda, and J. M. Dawson, Bull. Am. Phys. Soc. II, 17 (1972)1E7; also Cheng Chu, Ph.D. dissertation, Princeton University (1974).

[3]M. N. Rosenbluth and C. S. Liu, Fifth European Conference on Controlled Fusion and Plasma Physics, Grenoble, 1972, Vol. I, p. 12.

[4]T. H. Stix, The Theory of Plasma Waves (McGraw-Hill, New York, 1962), p. 225.

[5]M. Abramowitz and I. A. Stegun (Eds.), Handbook of Mathematical Functions (Dover, New York, 1965), p. 297.

[6]J. D. Jackson, J. Nucl. Energy C 1, 171 (1960).

[7]J. Canosa, J. Comput. Phys. 13, 158 (1973).

[8]J. Canosa, Phys. Fluids 15, 1536 (1972).

[9]K. O. Yngvesson and F. W. Perkins, J. Geophys. Res. 73, 97 (1968).

[10]H. B. Dwight, Tables of Integrals and Other Mathematical Data (Macmillan, New York, 1963), p. 239.

[11]S. Ichimaru and M. N. Rosenbluth, Phys. Fluids, 13, 2778 (1970).

[12]V. D. Shafranov, in Reviews of Plasma Physics, edited by M. A. Leontovich (Consultants Bureau, New York, 1967), Vol. 3, p. 144. The right-hand side of Eq. (15-24) of this reference can be shown to become $2\gamma_L T$ by calculating the average energy loss of the particles due to Cerenkov emission.

[13]S. I. Braginskii, in Reviews of Plasma Physics, edited by M. A. Leontovich (Consultants Bureau, New York, 1969), Vol. 1, p. 214.

[14]A. B. Langdon and C. K. Birdsall, Phys. Fluids 13, 2115 (1970); also H. Okuda and C. K. Birdsall, Phys. Fluids 13, 2123 (1970).

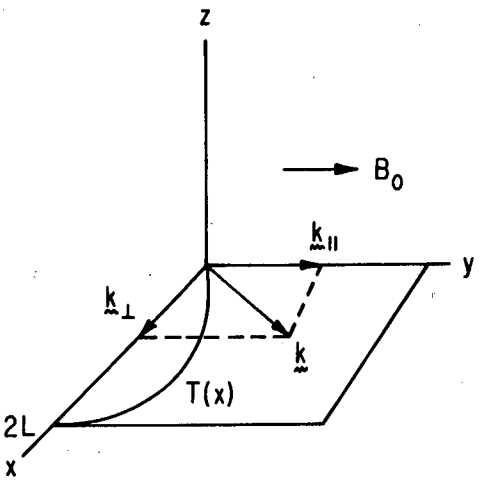

742132

Fig. 1. Illustration of the 2 1/2-dimensional particle model. In all the computations reported, we used 64 x 64 grids, 256 x 256 particles, $\lambda_D(L) = 2$, $L/\lambda_D(L) = 16$.

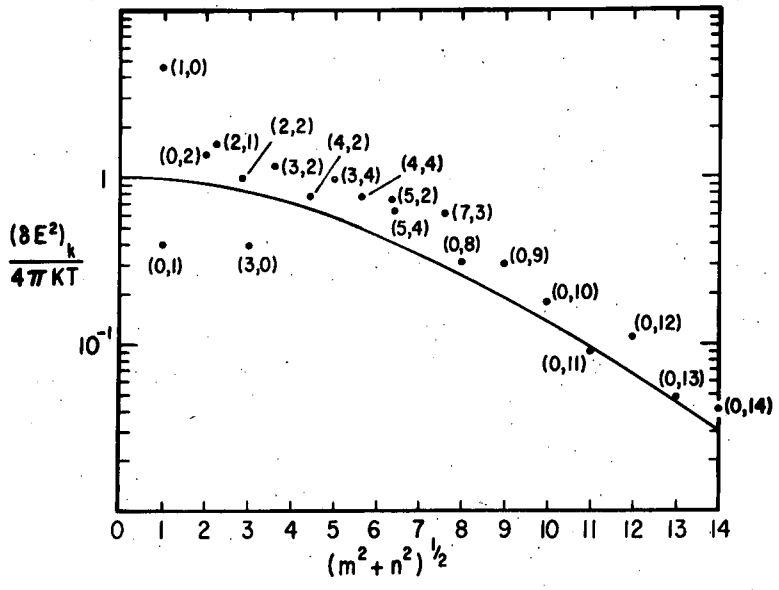

742129

Fig. 2. Measurement of the time-averaged fluctuation spectrum in k space. Time-averaged from $\omega_p t$ = 854 to 926; ω_p/ω_c = 1/4. Amplitudes of many modes are slightly higher than the equilibrium level due to the temperature gradient.

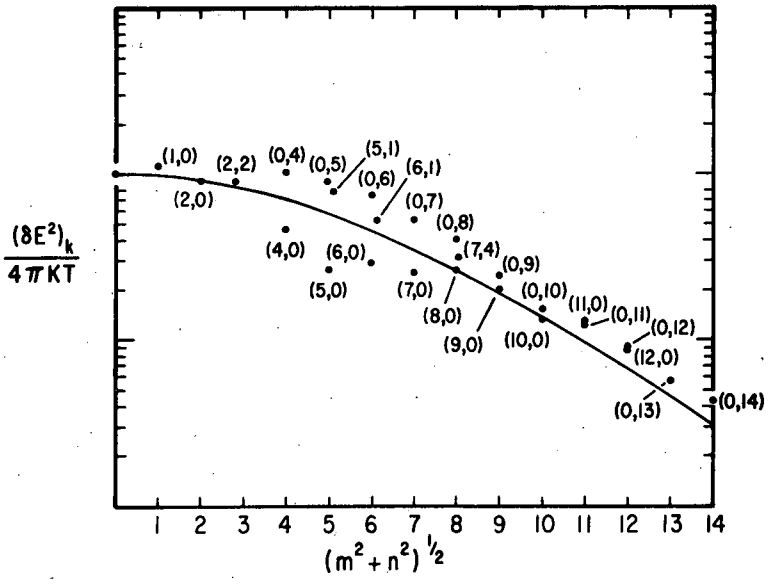

742123

Fig. 3. Measurement of the time-averaged fluctuation spectrum in k space. Time-averaged from $\omega_p t$ = 861 to 1019; ω_p/ω_c = 1.

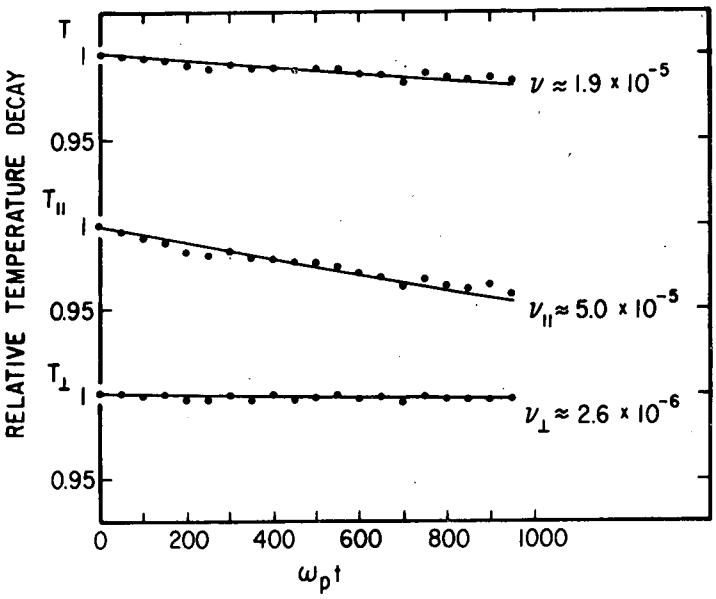

742126

Fig. 4. Relative temperature relaxation at the plasma center. T is the total temperature, $T = T_{\parallel} + T_{\perp}$, and the ν's are the experimentally determined slopes; $\omega_p/\omega_c = 1/4$. For very strong magnetic fields, the $T_{\parallel}$-decay is almost entirely due to wave transport and is considerably higher than the $T_{\perp}$-decay which is due to collisional transfer.

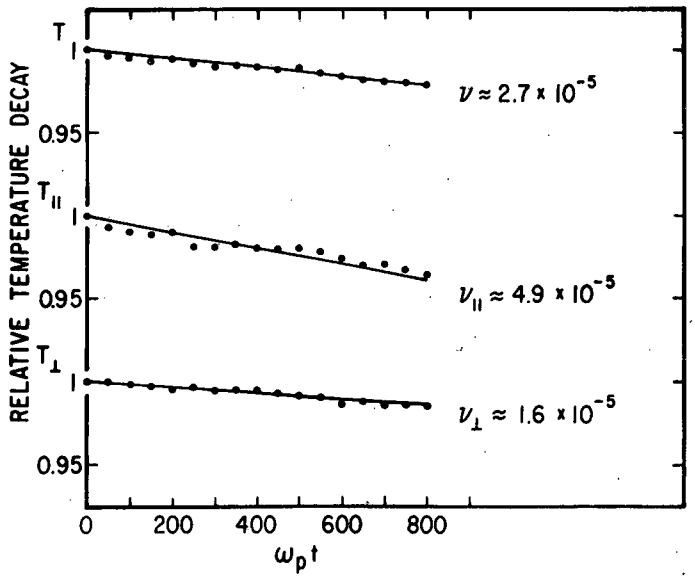

742127

Fig. 5. Relative temperature relaxation at the plasma center. $\omega_p/\omega_c = 1/2$. The contribution to the total temperature decay rate from wave transport is almost as high as that from collisional transport (see Table II).

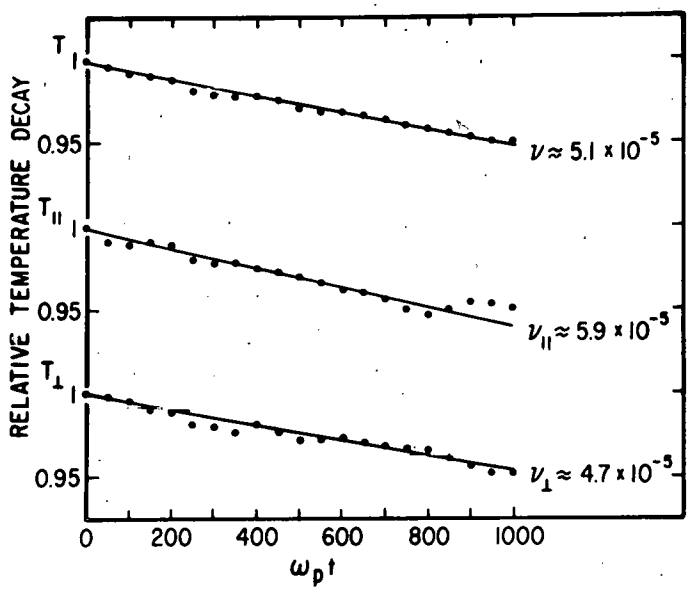

742131

Fig. 6. Relative temperature relaxation at the plasma center. $\omega_p/\omega_c = 1$. The total temperature decay rate is now mostly due to collisional transport (see Table II).

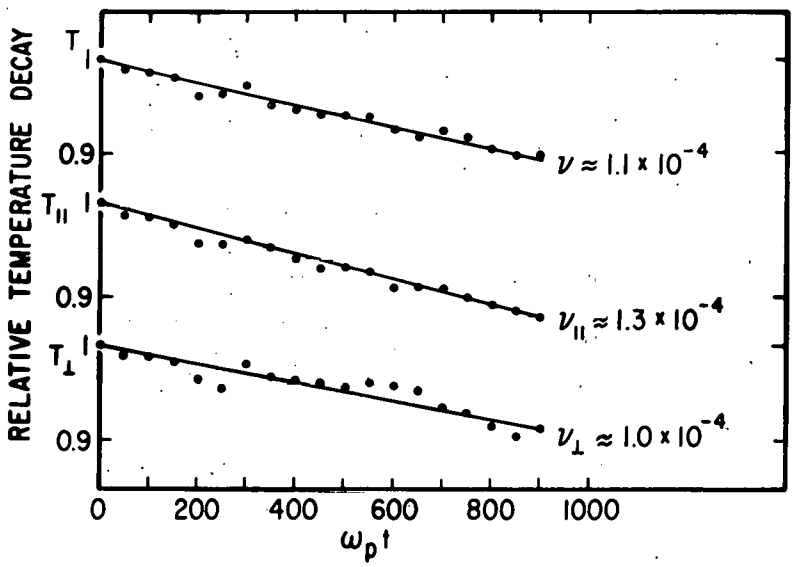

742130

Fig. 7. Relative temperature relaxation at the plasma center. $\omega_p/\omega_c = 2.5$. The total temperature decay rate is now mostly due to collisional transport (see Table II). Note the change in the vertical scale relative to the previous figures.

J. Gush